GEOMORPHOMETRY 2020 PERUGIA, ITALY JUNE 22 - 26 2020

4D geometrical and structural analysis of ground ruptures related to 2016 earthquakes in Sibillini mountains (Central Italy)

Marco Menichetti[1§], Daniela Piacentini[1], Emanuela Tirincanti[1], Matteo Roccheggiani[1]
[1]Dipartimento di Scienze Pure e Applicate, Università di Urbino, 61029, Urbino (PU)
[§] marco.menichetti@uniurb.it

Abstract—**3D multi-temporal reconstructions (4D) of the geometries and the kinematics of a portion of the 35 km coseismic surface ruptures related to 2016 Central Italy earthquakes are presented. The analysis integrates a traditional structural field survey with the data extracted from 3D point cloud models. These models were generated using a Structure-from-Motion (SfM) algorithms applied to georeferenced low-altitude aerial digital photos, both zenithal and oblique, acquired with small Unmanned Aerial Vehicles (UAV). Several comparisons were performed between data measured in the field and the same data detected on the point cloud models. The results show errors of a few cms, where models generally overestimate the real data. The coseismic ground ruptures typically show multiple overlapping scarps that can be divided into kinematic sets that occur throughout the width of the pre-existing SW dipping normal fault zones.**

I. Introduction

A detailed field mapping concerning the spatial geometries of the surface of coseismic ruptures belonging to active faults is the basis for the identification of seismogenic structures and represents an important step toward assessing the recurrence intervals and magnitude of earthquakes [1]. Data of fracture distributions, fault offsets, and links between geometries along the fault strands are the essential tools for extrapolating and constraining the depth of the fault plane from a kinematic point of view. Finally, kinematic fault analysis integrated with geophysical data, allowing to constrain any seismotectonic model.

Earthquakes producing coseismic surface deformation generate offsets in the landforms that are linked to the kinematics and the magnitude of the seismic events. Even though their importance in the seismic hazard assessment and subsequent reduction procedure, the accurate ground rupture morphologies, and their structural geometries remain uncertain. In many cases, the relevant extension of the coseismic ruptures and the morphologically complex landscape required long-time fieldwork to recognize and survey each strand of the fractures [1, 2].

The integration of geological and seismological data remains one of the main objectives for identifying active faults and assessing their potential hazard. While large data sets of instrumental seismological data are easy to gather, especially with modern digital seismic stations, field geological data remain very demanding in terms of human and economic resources, especially in remote areas. However, evolving technologies have allowed remotely sensed data to be used to obtain a lot of equivalent information. A complete and detailed survey of the geometries of coseismic ruptures is central to define the kinematic and the dynamic relationships of active faults and the regional seismic hazard [3].

A significant sequence of earthquakes occurred in the Sibillini mountains in Central Italy from August to October 2016. On August 24th, a Mw 6.1 earthquake struck the southernmost area between the town of Amatrice (Rieti province) and Arquata del Tronto (Ascoli Piceno province) (Fig. 1). Several ground ruptures along different strands of SW dipping extensional faults developed for more than 20 km in the M. Vettore area. The October 26th Mw 6.0 earthquake was centred in the Visso area (Macerata province), approximately 30 km northwest of the previous event. Following this event, only a few coseismic fractures have been surveying because, on October 30th, a new seismic event of Mw 6.5 occurred in the area near Norcia (Perugia province) [4]. This event occurred between the epicentres of the preceding earthquakes. It reactivated existing ground fractures and produced further ruptures over a larger area, including the northernmost sector of the Sibillini mountains, extend from the Tronto river valley in the south to the Chienti river valley in the north, over a distance of about 40 km (Fig. 1) [5, 6].

In this study, results of 3D multi-temporal reconstructions (4D) of the geometries and the kinematics of the coseismic surface ruptures are presented. These were obtained integrating a traditional structural field survey, with the data extracted from 3D point cloud models generated applying a Structure-from-Motion

Marco Menichetti, Daniela Piacentini , Emanuela Tirincanti and Matteo Roccheggiani (2020)

4D geometrical and structural analysis of ground ruptures related to 2016 earthquakes in Sibillini mountains (Central Italy):

in Massimiliano Alvioli, Ivan Marchesini, Laura Melelli & Peter Guth, eds., Proceedings of the Geomorphometry 2020 Conference, doi:10.30437/GEOMORPHOMETRY2020_39.

(SfM) algorithms to digital aerial low altitude photos. These images are a part of a larger dataset of more than 15k 2D zenithal and oblique aerial photos taken along 35 km of coseismic ruptures. This dataset was acquired using a small commercial remotely piloted aircraft, commonly referred as Unmanned Aerial Vehicle (UAV) or drone [6].

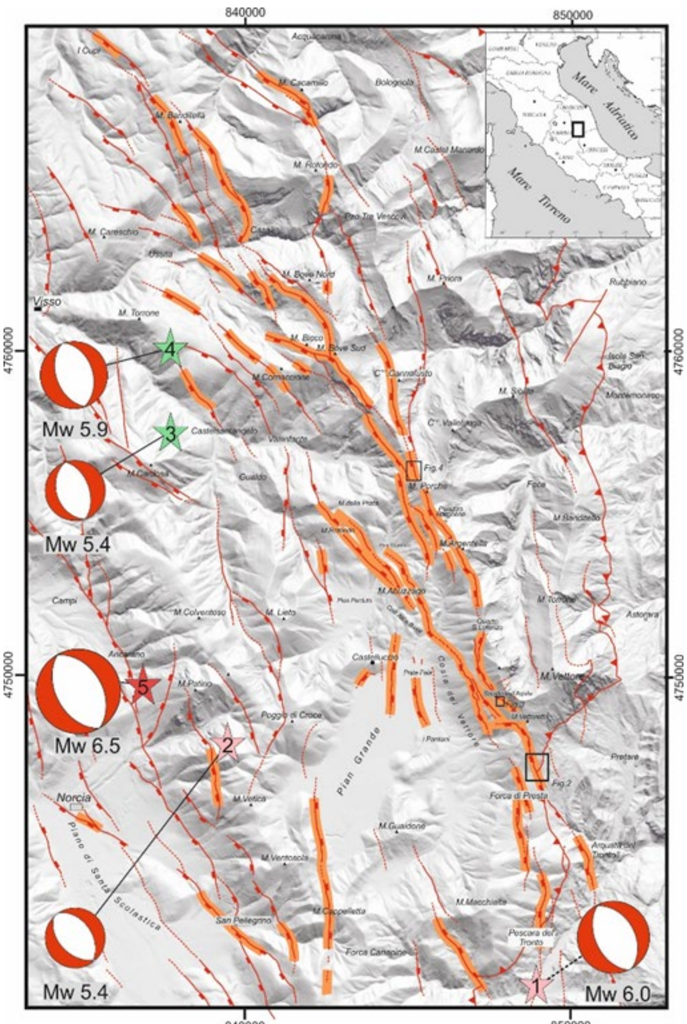

Figure 1. Structural map of the main Plio-Quaternary normal faults (barbs in the hw) and the Mio-Pliocenico Sibillini thrust (triangle in the hw). The seismic ruptures are highlighted in orange and the stars represent the epicenters of main earthquakes. Location of the study area is indicated in the box at the top right.

II. Methods

The in-field structural survey of the coseismic ruptures consists of acquiring the geometrical parameters, regularly sampled along each rupture strand, needed to define the spatial relationships between vertical and horizontal displacement. Usually in the field, these data are difficult to acquire, not only in the morphological complex and steeply mountain areas, because the apparent offset is normally measured. Moreover, structural analysis, paleoseismological studies, and quantitative geomorphological analysis need high-resolution terrain data (i.e., Digital Elevation Model) to characterize the landscape.

In the last years, a new generation of flying platform systems ready-to-use (i.e., like small UAVs with maximum weight < 25 kg) can acquire georeferenced low-altitude aerial digital photographs, both zenithal and oblique. The spatial camera position and orientation are determined by on board GNSS (Global Navigation Satellite System) units and by IMU (Inertial Measurement Unit) and geotagged on the photos together with other flight parameters.

At the same time, the photogrammetry techniques benefit of the new computer vision algorithms to transform 2D images into 3D topographic surfaces [7]. The Structure-from-Motion (SfM) algorithms are an alternative method of producing topographical data to respect the traditional stereo photogrammetry or airborne and terrestrial LiDAR [8]. The use of the photos limits the use of this technique in the vegetated area and therefore, the digital model of the terrain corresponds to the visible surface (Digital Surface Model - DSM). On the other hand, the possibility of combine oblique and zenithal photos both aerial and terrestrial permits to analyze the point cloud model from a different point of view and detect features otherwise invisible. A consumer-grade camera and the availability of commercial and open-source software where the SfM algorithms are implemented, allow producing accurate and georeferenced 3D points clouds, DSM, and orthomosaic [9]. Before planning a survey, it is necessary to define the required resolution (i.e., the size of the feature be resolved). This latter depends on the Ground Sampling Distance (GSD): pixel distance between two points. GSD is geometrically linked with the acquisition camera parameters (physical size of the sensor, resolution, and focal length) and the flight altitude or the distance from the object.

The accuracy and the precision of the generated points cloud can be improved exploiting the known sizes or the coordinates (X, Y, Z) of the objects visible in the utilized photos. Onboard, a Global Navigation Satellite System (GNSS) gives a decimeter precision, while spatial well-distributed Ground Control Points (GCP), with coordinates known with respect to a referenced system (i.e., UTM – WGS84), guarantee a centimeter accuracy. However, the precision and accuracy are influenced by environmental conditions, including wind, air temperature, and atmospheric moisture that also affect the GNSS receivers [7]. The survey of few km long strips in the steep mountain slopes where the seismic ruptures are localized presents various problems for georeferencing the model. The use of objects with known size has been preferred respect to position and measure the GCP. The derived point clouds have a good precision (centimeters), and low accuracy (meters) respects the geospatial reference frames. For each 3D cloud model, the possible survey errors, including reprojection and camera location errors are known and consistent with the size of surveyed features [8].

Several checks and comparison were performed between data of offset measured in the field and the same data detected on the point cloud model. The results show errors of a few cm, less 5%, where the model generally overestimates the real data. Finally, the quality of the topographic and geological 3D point clouds can be improved using several techniques including editing, resampling as well as, using different reprocessing methods or filters.

During the second semester of the 2016 and the 2017, along 35 km of coesismic ruptures, we used two commercial quadcopter drones to acquire more than 15k, 2D zenithal and oblique aerial photos. These platforms are equipped with a stabilized camera mount, producing geotagged photos in RAW format, georeferenced through two GNSS units (GPS and GLONASS) located above the camera gimbal. The model DJI Phantom 3 Pro equipped with a Sony sensors Exmor of size of 1/2.3" with a calibrated FOV 94°, 20 mm f/2.8 lens allows photo resolution of 12.76 Mpixel. The model DJI Phantom 4 Pro equipped with a Sony sensors Exmor of size of 1" with a calibrated FOV 84°, 24 mm f/2.8 lens allows photo resolution of 20 Mpixels.

The digital images were processed using Structure from Motion algorithms obtaining eighteen 3D point cloud models with more 10^7 points for each area. These were generated, including DSM and orthomosaics with centimeter resolution (Fig.2).

These point clouds permitted to generate a fully rendered 3D DSM where the geological structures, like faults and fractures and the displacements of several centimeters, can be easily traced and measured. From the microtopography map, features such as small water channels, upper and lower slope angles are easily detected and quantitatively analyzed. The attitude of these discontinuities, expressed by offset, dip direction and dip, was measured using a combination of GIS tools, integrated and verified with the digital field survey checks, and subsequently processed via the traditional geometrical spatial methods using structural statistical tools.

Some areas, especially in the M. Vettore sector (Fig. 3), were surveyed before and after the October 30 event, making possible a 4D kinematic reconstruction of the coseismic ruptures. Comparison of the multi-temporal point clouds in fact permit to define the kinematics of the fault strands for each of the two main earthquake events (Fig. 4).

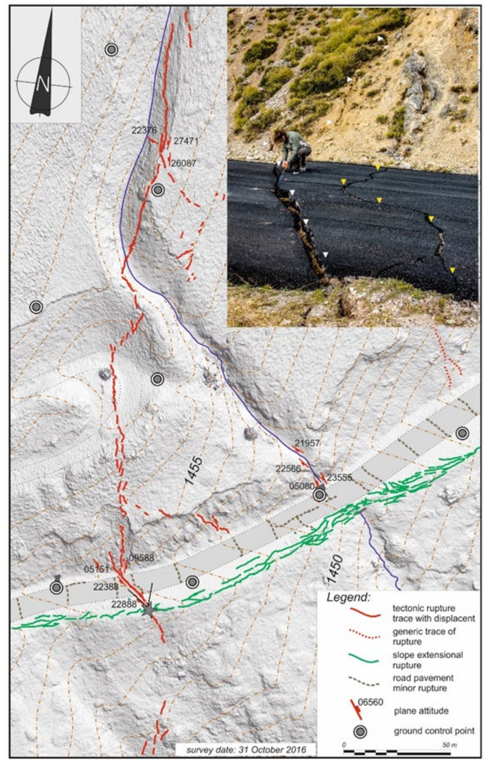

Figure 2. Digital surface model (DSM) with a resolution of 2 cm/pixel, of the SSE slope of M. Vettoretto, along the road SP 477. The contour lines refer to the orthometric height (EGM96 – geoid H 47.251 m). In the photo (taken in the point represented with the grey star) the offset within the road pavement of about 13 cm is observable; the white triangles indicate the coseismic ruptures of the October 30 2016 earthquake, while the yellow triangles indicate the reactivation of the August 24 coseismic ruptures. Location of the area is shown in Fig.1.

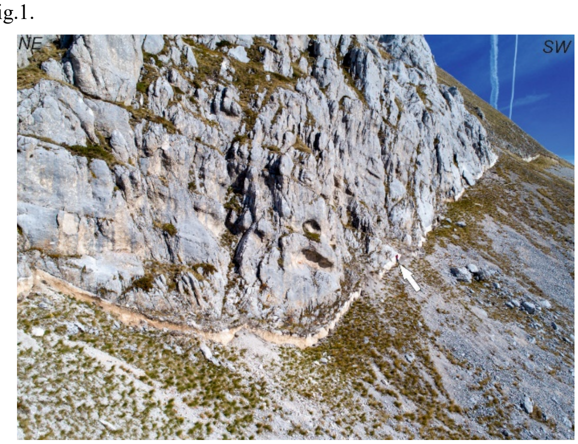

Figure 3. Oblique aerial view of the M. Vettore rupture. The arrow indicates a person. Location of the area is shown in Fig.1

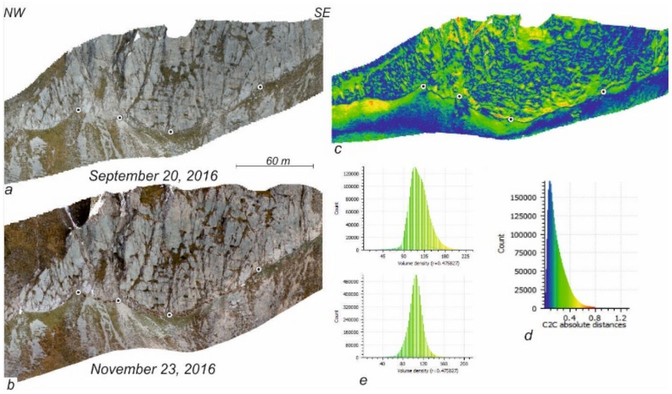

Figure 4. 3D point clouds of a portion of M. Vettore ruptures acquired on September 20, 2016 (a) and on November 23, 2016(b). Dotted circle are the GCP. In (c) the 4D point cloud derived comparing the two dataset. The graphs show the distribution of the absolute distance between the two clouds (d) and the volume density distribution for each point cloud (e). Location of the area is shown in Fig.1.

III. Results and conclusions

The along-strike displacement versus distance of the fault planes and ground ruptures was analyzed along several cross-sections. The surface ruptures generally crossing the already known normal faults. They have a continuous extent of ~35 km and consist of open cracks and vertical dislocations or warps (2 m maximum throw) orientated NW-SE (Fig. 5). At least 12 fault strands SW dipping, with an average angles of 65°, and whose geological offsets are many hundred meters have been surveyed. Four reactivated ground ruptures NE dipping, less steep than the normal fault, and whose geological offsets are few hundred meters have been also observed. Structural relations such as fracture length and distributions, fault offsets, shear zone width, links between geometries along the fault strands provide insight regarding the mechanics of earthquake rupture. These parameters are the input for any seismic-hazard analysis, engineering design criteria, and studies of fault rupture dynamics. The extension and distribution of the coseismic fault slip in the near-surface give insight into the initiation, propagation, and cessation of dynamic ruptures and the structural evolution of the faults. The distribution and internal configuration of the rupture zones often display complex structures comprising two or more anastomosing, synthetic slip-surfaces. Looking in three dimensions, the degree of complexity is seen to vary, and parts of a rupture zone with multiple slip-surfaces can alternate with parts with a single surface. These ruptures typically show multiple overlapping scarps that can be divided into kinematic sets that occur throughout the width of the pre-existing fault zones. The spatial variation records the evolution of the fault zone with more complex structures arising from several processes including a linkage between different rupture segments, which shows to be a common fault growth mechanism.

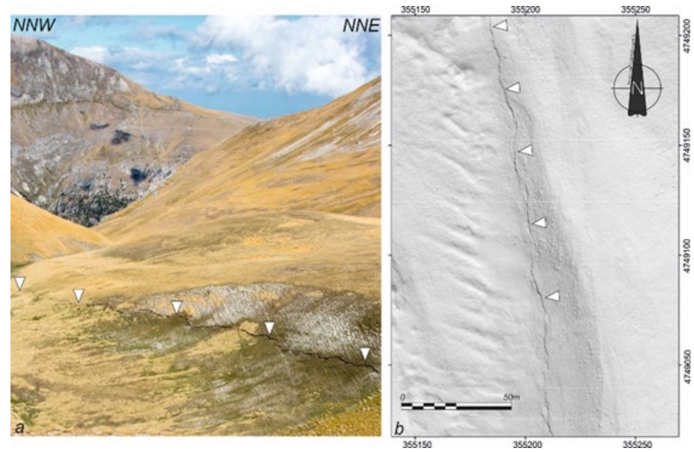

Figure 5. Aerial oblique view of the eastern slope of the M. delle Porche where coseismic ruptures of October 30, 2016 are visible (a) and the DSM (EPSG 32633) of the same area (b). The white triangles represent the shared points between the two images. Location of the area is shown in Fig.1.

References

[1] Scholz, C., 2002. "The Mechanics of Earthquakes and Faulting". Cambridge University Press. doi:10.1017/CBO9780511818516.008.

[2] McCalpin J., 2009. "Paleoseismology". International geophysics Elsevier, vol. 95, 613 p.

[3] Menichetti, M., D. Piacentini, F. Troiani, G. Guidotti, A. Napolitano, 2016. "Remote sensing investigation techniques for the analysis of rocky slope stability in remote areas: a test from the Sierra Madre Occidental, Mexico." Rend. Online Soc. Geol. It., 39, 113-116.

[4] Chiaraluce, L., R. Di Stefano, E. Tinti, L. Scognamiglio, M. Michele, E. Casarotti, M. Cattaneo, P. De Gori, C. Chiarabba, G. Monachesi, A. Lombardi, L. Valoroso, D. Latorre, S. Marzorati, 2017. "The 2016 Central Italy seismic sequence: a first look at the mainshocks, aftershocks, and source models". Seismol. Res. Lett., 88(3), 757–771.

[5] Civico, R., S. Pucci, F. Villani, L. Pizzimenti, P.M. De Martini, R. Nappi, R., the Open EMERGEO Working Group, 2018. "Surface ruptures following the 30 October 2016 Mw 6.5 Norcia earthquake, central Italy". Journal of Maps, 14:2, 151-160.

[6] Roccheggiani, M., A. Tamburini, E. Tirincanti, M. Menichetti, 2018. "Automated detection of surface ruptures associated with the 2016 Central Italy earthquake sequence by Sentinel-1 SAR interferometry data". Proceedings of the 9th International INQUA meeting on Paleoseismology, Active Tectonics and Archeoseismology, 229-232.

[7] Carbonneau, P.E., J.T. Dietrich, 2017. "Cost-effective non-metric photogrammetry from consumer-grade sUAS: implications for direct georeferencing of structure from motion photogrammetry". Earth Surf. Process. Landforms, 42, 473– 486.

[8] Turner, D., A. Lucieer, C. Watson, 2012. "An automated technique for generation georectified mosaics from ultra-high resolution Unmanned Aerial Vehicle (UAV) imagery, based on structure from motion (SfM) point clouds". Remote Sens., 4, 1392–1410.

[9] Westoby, M.J., J. Brasington, N.F. Glasser, M.J. Hambrey, J.M. Reynolds, 2012. "Structure-from-Motion' photogrammetry: A low-cost, effective tool for geoscience applications". Geomorphology, 179, 300–314.